Biodistribution Investigations of Technetium-Labelled Murine Bone Marrow-Derived Extracellular Vesicles by Nanospect/Ct

ANDREA BALOGH[1,#], ANDRÁS POLYÁK[1,2,#], ADRIENN ZSANETT PÉTERI[1], ANETT BENEDEK[1], ZITA PÖSTÉNYI[1], LÍVIA NASZÁLYI NAGY[3##], LAJOS BALOGH[1], ESZTER PERSA[1], GÉZA SÁFRÁNY[1], MUNIRA KADHIM[4], KATALIN LUMNICZKY[1*]

[1] National Public Health Centre – National Research Directorate for Radiobiology and Radiohygiene, Budapest, Anna u. 5, Budapest, 1221, Hungary;

[2] Department of Nuclear Medicine, Hannover Medical School, Carl-Neuberg Str 1, 30625 Hannover, Germany;

[3] Institute of Materials and Environmental Chemistry, Research Centre for Natural Sciences, Hungarian Academy of Sciences, Budapest, Magyar Tudósok Blvd 2, Budapest, 1117 Hungary;

[4] Genomic Instability Group, Department of Biological and Medical Sciences, Oxford Brookes University, Gipsy Lane, Oxford OX3 0BP, UK

[#]These two authors contributed equally to this work.

[##] Current address: Research Group for Molecular Biophysics, Hungarian Academy of Sciences-Semmelweis University H-1094 Budapest, Tűzoltó u. 37-47 Hungary

Abstract

The *in vivo* tracing of the biodistribution of extracellular vesicles (EVs) is a pre-requisite in identifying their target cells and understanding their function. Although fluorescent labelling of EVs is already used, radiolabelling can provide more details in understanding biodistribution of EVs. In the present paper we report radiolabelling of bone marrow-derived EVs and *in vivo* tracing of their biodistribution. EVs isolated from the bone marrow supernatant of C57BL/6 mice were labelled with the technetium-99m (^{99m}Tc) isotope. Labelling was efficient and labelled EVs were stable during the 24 hours follow-up. Detection of labelled EVs after intravenous injection in mice was performed using *ex vivo* measurements and *in vivo* imaging. *Ex vivo* examinations revealed that at 4 hours post-injection, the highest accumulation rate was in the liver, kidney, spleen and femur epiphysis. *In vivo* imaging using nanoSPECT/CT confirmed the *ex vivo* examinations and demonstrated slow elimination of the radioactivity, 24 hours post-injection the bone marrow-containing epiphysis and lymph nodes showed the highest retention values; liver, spleen and kidney were also clearly detectable. In summary, labelling of bone marrow-derived EVs with ^{99m}Tc coupled with SPECT/CT detection was a reliable method for quantitative distribution studies of EVs *in vivo*.

Key Words: extracellular vesicle, irradiation, NanoSPECT/CT, bone marrow, murine model, Technetium

ABBREVIATIONS:

AChE: acetylcholinesterase;

CT: computed tomography;

DLS: dynamic light scattering;

EV: extracellular vesicle;

HMPAO: hexamethylpropyleneamineoxime;

MV: microvesicle;

PET: positron emission tomography;

SPECT: single photon emission computed tomography;

SUV: standardized uptake value;

^{99m}Tc: technetium-99m;

TLC: thin layer chromatography;

INTRODUCTION

Extracellular vesicles (EVs) are membrane vesicles released by different cell types. Based on their size and biogenesis EVs are divided into the following groups: exosomes released by multivesicular bodies upon cellular membrane fusion with a diameter of 50-100 nm, microvesicles (MVs) formed by membrane budding with a diameter of 20-1000 nm, and apoptotic bodies released during apoptosis with a diameter of up to 5000 nm in diameter (van der Pol et al., 2012; Andaloussi et al., 2013). Exosomes and MVs have prominent roles in intercellular communication by transferring genetic material (in the form of mRNA and miRNA) and various proteins to neighbouring and distant recipient cells (Hurley et al., 2010).

Corresponding author: Katalin Lumniczky, M.D., Ph.D.,
National Public Health Center
National Research Directorate for Radiobiology and Radiohygiene,
Anna u. 5, Budapest, H-1221, Hungary.
Phone: (+36) 1-4822011
E-mail: lumniczky.katalin@osski.hu

Received: 17th October 2016
Accepted: 15th November 2016

The *in vivo* tracing of the biodistribution of EVs is a pre-requisite in identifying their target cells and understanding their function. EVs might also provide a future therapeutic method for drug delivery (van Dommelen et al., 2012), and in this regard, it is essential to characterize their distribution kinetics, homing and cellular uptake. High-resolution nuclear imaging methods like PET (positron emission tomography) and SPECT (single photon emission computed tomography) combined with radiolabelled molecules targeting specific cell surface proteins offer a powerful tool with high detection sensitivity and spatial resolution for various morphological, functional and biodistribution studies. Combining the information obtained from functional SPECT along with anatomical computed tomography (CT) data increases the diagnostic and research power of scintigraphy (Franc et al., 2008) in various pathophysiological conditions in the field of cardiovascular diseases (Golestani et al., 2010) or oncology (Polyak et al., 2013). For SPECT/CT imaging investigations, the most frequently applied tracer isotope is the technetium-99m (^{99m}Tc). ^{99m}Tc-radiolabelling of a high number of different compounds and biomolecules are described in the literature such as different proteins (Honda et al., 1970; Rhodes, 1991), newly developed polymers (Polyak et al., 2013) and liposomes (Anghileri et al., 1976) as well.

In the present study we report radiolabelling of bone marrow derived EVs with ^{99m}Tc isotope and monitoring their distribution and pharmacokinetics by nanoSPECT/CT imaging system after intravenous injection in mice.

MATERIALS AND METHODS

Isolation of EVs

Eight weeks old C57BL/6 mice were used for the experiments. Mice were kept and investigated in accordance with the guidelines and all applicable sections of the Hungarian and European regulations and directives. All animal studies were approved and permission was issued by Budapest and Pest County Administration Office Food Chain Safety and Animal Health Board. Bone marrow was harvested in PBS by flushing out the bone marrow from the femurs and tibias of 8 male C57/BL6 mice. Single cell suspension was made of bone marrow by mechanical disaggregation of the tissue. Intact, viable cells were pelleted and separated while the bone marrow supernatant was used for exosome isolation. EVs were isolated using the ExoQuick-TC™ kit (System Biosciences, CA, USA) according to the manufacturer's protocol. In brief, the bone marrow supernatant was incubated with ExoQuick-TC™ solution at 4°C overnight and centrifuged at 1500 x g for 30 minutes. The supernatant was aspirated and the residual solution was spun down by centrifugation at 1500 x g for 5 minutes. The pellet was resuspended in 200 µl of PBS. For removal of residual ExoQuick polymers the EV solution was passed through a PD SpinTrap G-25 desalting column (GE Healthcare, Life Sciences, WI, USA) following the manufacturer's protocol. Protein content of EVs was measured using the Bradford protein assay kit (Sigma-Aldrich, MO, USA). EV-associated acetylcholine-esterase activity was determined in EV solution with increasing EV amount using the Acetylcholinesterase Assay Kit (Abcam, Cambridge, UK) over a time period of 30 minutes by following absorbance at 410 nm with a plate reader (BioTek, USA).

Characterization of EVs by dynamic light scattering and flow cytometry

The hydrodynamic size and polydispersity of EVs were determined by the dynamic light scattering (DLS) method using an Avid Nano W130i DLS instrument (High Wycombe, UK). For flow cytometry analysis, EVs (20-30 µg) were incubated with 6 x 10^6 4-µm diameter aldehyde/sulphate latex microbeads (Life Technologies) in a final volume of 100 µl of PBS at room temperature for 15 minutes. The volume was made up to 400 µl and incubated on a rotator at 4°C overnight. After the incubation the reaction was stopped by the addition of 100 mM glycine for 30 minutes to block remaining free binding sites. EV-coated beads were washed in PBS twice and stained with APC conjugated CD9 antibody (Molecular Probes, OR, USA) or isotype control (Beckton Dickinson, NJ, USA). Samples were analysed on a FACScalibur flow cytometer (Beckton Dickinson) using CELL-Quest Pro data acquisition and analysis software (Beckton Dickinson).

Labelling with ^{99m}Tc

^{99m}Tc-pertechnetate ($^{99m}TcO^{4-}$) was derived from an UltraTechnekov (10.75 GBq) ^{99}Mo-^{99m}Tc generator (Covidien Imaging Solutions, USA). Prior to labelling, a 40 µl aliquot of the isolated EV-PBS suspension was completed to 200 µl volume by the addition of sterile 0.9% (w/v) NaCl solvent (Salsol). Then 440 MBq activity of sterile generator-eluted $^{99m}TcO^{4-}$ in 200 µl Salsol and 2 µl of 5 mg/ml $SnCl_2$ (x $2H_2O$) in 0.05 M HCl was added to the EV suspension. The ^{99m}Tc-labelling reaction was performed by incubation at room temperature for 20 minutes. The labelling efficiency was assessed by thin layer chromatography (TLC) using ITLC-SG plates (Agilent Technologies, CA, USA) and methyl ethyl ketone (Reanal Ltd., Budapest, Hungary) as eluent for 20 minutes, 2 and 24 hours postlabelling.

Biodistribution studies

For biodistribution studies 5 µg EVs labelled with $^{99m}TcO^{4-}$ (20 MBq activity) was injected into the tail vein of C57Bl/6 mice. Distribution of the radiolabelled EVs was determined in two ways: by *ex vivo* measurements, when mice were sacrificed, various organs were removed and the activity of the individual organs was determined *ex vivo* in a gamma scintillation counter and by *in vivo* measurements when the distribution of the radioisotope was determined in live animals by nanoSPECT/CT scanning.

Ex vivo biodistribustion measurements were carried out 4 hours after the injection of radiolabelled EVs. C57/BL6 mice (n=5) were sacrificed by cervical dislocation, blood was collected, and organs of interest (thymus, heart, lungs, stomach, liver, spleen, kidneys, femur, bone marrow, muscle, lymph node, brain) were dissected, rinsed and weighed. The epiphysis of the femur was removed approximately at the metaphysis and the bone marrow was flushed from the diaphysis. Radioactivity in various organs was measured in a Nal(TI) crystal gamma scintillation counter (NZ-310, Gamma, Hungary). Percentages of radioactivity dose administered per gram organ (% ID/g) were determined.

For the *in vivo* nanoSPECT/CT imaging investigations, three C57/BL6 mice were injected with the same amount of radiolabelled EVs as for the *ex vivo* measurements. *In vivo* imaging and analysis was performed by the CROMed LTD (Budapest, Hungary). Animals were anesthetized with 2% isoflurane in oxygen during the SPECT/CT measurements. Imaging was performed 3 and 24 hours post-injection on a nanoSPECT/CT PLUS (Mediso Ltd., Hungary) instrument and data were analysed with Interview Software (Mediso Ltd.). The standardized uptake value (SUV) was defined as the ratio of the radioactivity within a region of interest and the amount of injected radioactivity after decay-correction divided by the body weight.

RESULTS

Validation and in vitro characterization of bone marrow-derived EVs.

The measured hydrodynamic mean diameter of the isolated EVs was 248.52 nm (SD = ± 145.95 nm) *(Fig. 1A)* with a relatively high polydispersity (Polydisp = 58.73) indicating a heterogeneous EV composition, formed mostly by MVs and to a lesser extent by exosomes.

In order to further characterize the isolated EVs two parameters specific for both exosomes and MVs were investigated: the acetylcholinesterase (AChE) activity of the EVs and the level of CD9 expression on the surface of EVs by flow cytometry. The measured AChE activity is shown in *Figure 1B*, where it can be seen that enzyme activity is proportional with the amount of microparticles. Flow cytometric characterization of bone marrow-derived EVs showed a more than 70% expression of the CD9 tetraspannin, a membrane-bound molecule used as a specific marker for both exosomes and MVs *(Figure 1C)*.

Figure 1.

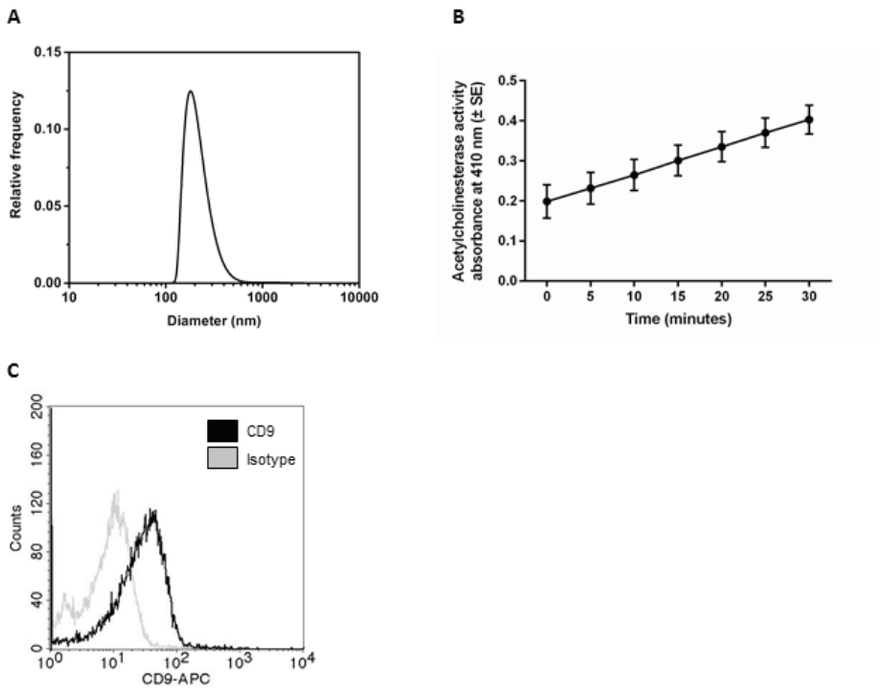

Figure 1. Characterization of bone marrow-derived EVs. **A**. Particle size distribution of isolated EVs measured by the DLS method. **B**. Acetylcholinesterase activity of EVs measured over 30 minutes. Values represent the mean of three samples ± SD. **C**. Expression level of the CD9 marker measured by flow cytometry using EV coupled to latex beads.

^{99m}Tc-radiolabelling of EVs showed a high labelling efficiency as determined by TLC analysis. The fraction of labelled EVs was more than 98% 20 minutes after labelling, it changed minimally 24 hours later (93%) and dropped to 85% by 48 hours after labelling *(Table I)*. This indicates that direct radiolabelling of EVs with ^{99m}Tc was efficient and was stable for a minimum of 24 hours.

Table I.

Efficiency and stability of labelling of bone marrow-derived EVs with ^{99m}Tc

Sample	Fraction of ^{99m}Tc-labelled EVs (%)
EVs 20 minutes after labelling	98.23 (± 1.25)
EVs 24 hours after labelling	93.14 (± 5.14)
EVs 48 hours after labelling	85.62 (± 12.6)

In vivo biodistribution of bone marrow derived EVs

The biodistribution studies of the radiolabelled EVs were performed by *ex vivo* measurement of the radioactivity of different organs and by *in vivo* measurements based on SPECT/CT images. The animals tolerated the i.v. applications well, no clinical side effects could be observed during the time course of the examinations. During the *ex vivo* biodistribution study various organs were harvested 4 hours post-injection and the radioactivity of each organ was determined. The % ID/g values obtained for the organ activity uptakes are presented in *Figure 2A*. The highest uptake was measured in the liver with 11.49% ID/g (SD = ± 2.22%) representing 32.5% of the total injected radioactivity. A lower level of radioactivity was present in the lungs and spleen with 3.51 % ID/g (SD = ± 1.11%) and 2.88% ID/g (SD = ± 0.83%) respectively. Surprisingly high uptake was detected in the femur, representing 22% of the total injected activity, and resulting in 2.50% ID/g (SD = ± 0.16%) activity of the bone. Further analysis revealed that the bulk of this activity was located in the epiphyses of the femurs *(Fig. 2B)* while the diaphysis contributed with a much lower rate to the entire activity of the intact femur. A retained blood-background could be concluded which could relate to a relatively long circulation time of the injected EVs. The activity ratio in the thyroid and stomach was negligible indicating the stability of radiolabelling after i.v. application. The brain did not show any significant uptake.

Figure 2.

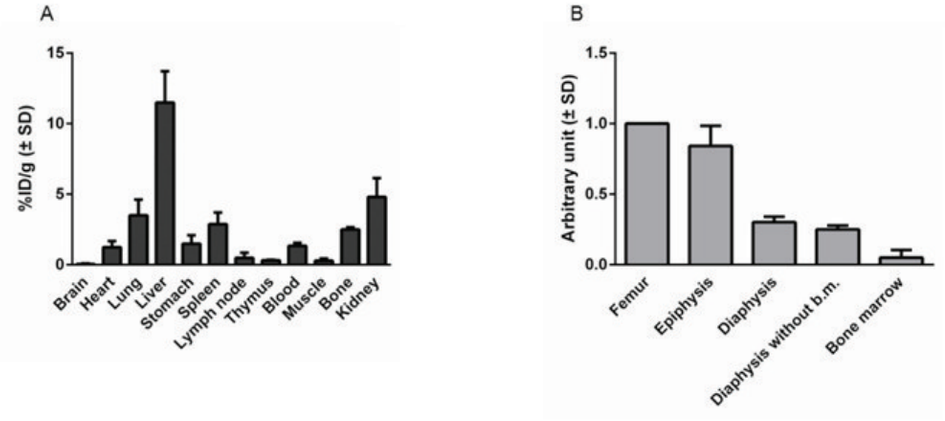

Figure 2. Biodistribution of ^{99m}Tc-labelled EVs quantified *ex vivo*. **A**. Biodistribution of ^{99m}Tc-labelled EVs showing %ID/g values in C57/BL6 mice (n=5) 4 hours post injection. **B**. Distribution of radioactivity in the femur. Arbitrary units represent percentage of the total radioactivity detected in the femur. Data represent the mean of four measurements ± SD.

The *in vivo* biodistribution studies performed with the whole-body SPECT/CT scans 3 and 24 hours after EV administration showed comparable results with the *ex vivo* measurements *(Fig. 3A, B, C, D, E)*. The weak signal detected in the thyroid gland and the gastrointestinal system at both time points of the measurements confirms the high degree and stability of the labelling, as these organs are known to accumulate mainly free ^{99m}Tc isotope *(Fig. 3E*). The urinary system, which is the main elimination route of the free isotope, radiolabelled protein fraction and products of the degraded EVs, displayed increased uptake 3 hours post-injection, which decreased by 24 hours post-injection. Strong accumulation of the EVs was visible in the liver, lungs and spleen as soon as 3 hours post-injection while slightly decreasing over the 24 hour follow-up period. Small but persistent uptake was detected in the lymph nodes. In line with the *ex vivo* biodistribution, the nanoSPECT/CT scans showed high uptake of the radiolabelled EVs in the epiphysis of the femurs *(Fig. 3E)*. Comparing the SUVs measured at 24 hours with the SUVs measured at 3 hours post-injection, the tissue retention value was calculated *(Fig. 3F*), indicating how long the radioactivity persisted in the tissues. The highest tissue retention values were seen in the bone, epiphysis and lymph nodes, where the injected radioactivity detected 24 hours post injection was more than 80% for bone and epiphysis and above 70% for lymph nodes. The lungs, liver and spleen were still clearly visible on the scans retaining approximately 60% of the injected radioactivity. The bulk of the radioactivity was excreted through the urinary system with a retention value of 40% in the kidney and 20% in the bladder. In conclusion, both *ex vivo* and *in vivo* biodistribution studies showed that apart of accumulating in the liver and lungs a substantial amount of the EVs were present in the epiphysis of the femurs rich in red bone marrow and in the lymph nodes and spleen, indicating stable accumulation of bone marrow-derived EVs in the haematopoietic tissue.

Figure 3.

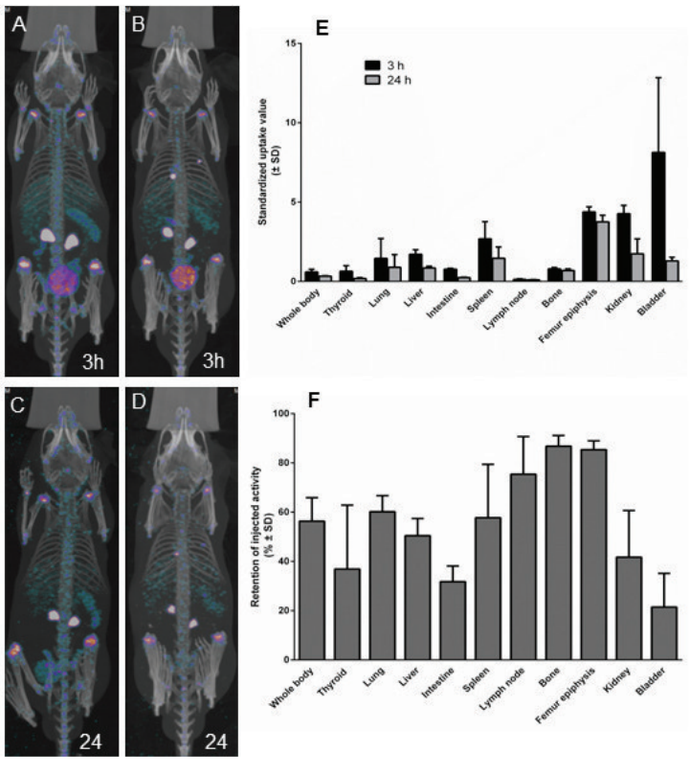

Figure 3. Biodistribution of ^{99m}Tc-labelled EVs based on *in vivo* quantification. **A., B.,C.,D**. Representative nanoSPECT/CT images of C57/BL6 mice 3 hours (A, B) and 24 hours (C, D) post-injection of ^{99m}Tc-labelled EVs. **E**. Biodistribution of ^{99m}Tc-labelled EVs based on SUV values in C57/BL6 mice (n=3) 3 and 24 hours post injection. **F**. Retention values represent the activity at 24 hours as the percentage of the initial activity measured at 3 hours post-injection. Data represent the mean of 3 measurements ± SD.

DISCUSSION

In the present study we describe ^{99m}Tc radiolabelling of murine bone marrow-derived EVs and characterize their biodistribution and pharmacokinetics in recipient mice with nanoSPECT/CT imaging system.

To date there are few published studies focusing on the biodistribution and pharmacokinetics of various EVs. Most of them apply *in vivo* or *ex vivo* imaging preceded either by cell transfection in order to introduce the reporter gene into the EV releasing cell or by labelling the EVs with fluorescent dyes (Takahashi et al., 2013, Morishita et al., 2015, Wiklander et al., 2015). The transfection approach restricts the applicability of the method to easily transfectable cell lines, making it difficult or almost impossible to employ it in biodistribution studies of EVs of primary cell origin. Even though the use of fluorescent lipophilic dyes can replace the use of marker genes, and thus eliminates the transfection step, the lower sensitivity of the *in vivo* imaging systems used to detect either luminescence or fluorescence imposes further limitations to its applications. In a recent study Wiklander et al. reported the use of a fluorescent lipophilic tracer-DiR to label EVs followed by *ex vivo* imaging to study the biodistribution of EVs (Wiklander et al., 2015). Morishita et al. in order to improve the detection sensitivity radiolabelled exosomes derived from B16BL6 tumor cell line with iodine-125 (^{125}I) based on streptavidin-biotin system

(Morishita et al., 2015). Again, this method required the transfection of the exosome releasing cells with a plasmid vector encoding the fusion protein streptavidin-lactadherin in order to bind the ^{125}I-labelled biotin.

Performing ^{99m}Tc labelling of EVs and using SPECT/CT for biodistribution measurements overcomes several of the above mentioned problems. In a recent paper Hwang et al. (2015) has reported radiolabelling and biodistribution analysis of exosome-mimetic nanovesicles isolated from the mouse RAW264.7 macrophage cell line with ^{99m}Tc-hexamethylpropyleneamineoxime (HMPAO). While the ^{99m}Tc-HMPAO labelling method relies on the penetration of the highly lipohilic ^{99m}Tc-HMPAO into the cell, where it is converted to hydrophilic form and is retained inside the cell, we used the direct labelling method with ^{99m}Tc, which is a one-step labelling process where the technetium binds to bisulphide groups in the proteins present on the surface of EVs (Rhodes, 1991). The two labelling methods were comparable in terms of labelling efficiency. A major difference though was the nature of particles used for radiolabelling. Hwang et al. used exosome-mimetic nanovesicles obtained by the breakdown of macrophage cells, while we used unmanipulated EVs purified directly from the freshly isolated bone marrow supernatant of mice. Hwang et al. performed SPECT/CT scans to show distribution of the radioactivity but quantified the amount of radioactivity accumulated in the various organs *ex vivo*. We performed both *ex vivo* quantification of radioactivity distribution and also direct SPECT/CT analysis for quantitative distribution and pharmacokinetics measurement. This latter analysis was based on standardized uptake value calculation, a common parameter also used in human SPECT/CT investigations for biodistribution studies of radioisotopes. Basically, in accordance with the Hwang data, we found the highest accumulation in the liver, and a substantial amount of radioactivity was detected in the kidney, spleen and lungs as well. However, we could show higher amount of radioactivity in the bone than Hwang et al. Further analysis of bone radioactivity revealed that most of it was present in the epiphysis indicating accumulation of labelled EVs in the bone marrow. Additionally, we could also show low but detectable accumulation in peripheral lymphoid organs other than spleen such as thymus and lymph nodes. This distribution pattern could be confirmed by the direct SPECT/CT quantification also, where epiphysis were the organs with the highest SUV values.

A key point in the biodistribution of EVs of different cellular origin is to what extent their uptake is cell- or tissue-specific. Imai et al. (2015) using macrophage depleted mice demonstrated that the main clearance route of intravenously administered exosomes was through macrophages residing in the liver and spleen. The fact that most of the *in vivo* and *ex vivo* biodistribution studies (Morishita et al., 2015, Wiklander et al., 2015, Hwang et al., 2015), including ours show high uptake levels in the liver and spleen are indirect evidences that macrophages play important role in EV clearance. On the other hand, this does not exclude the possibility that targeted uptake is also present via specific homing receptors which influence EV biodistribution. It has been shown by Saunderson et al. (2015) that sialoadhesin (CD169) bearing macrophages in the spleen and lymph nodes were responsible for uptake of primary B cell-derived exosomes via surface expressed 2,3 linked sialic acids.

In conclusion, in the present study we showed that EVs isolated directly from bone marrow represent a heterogeneous population of vesicles concerning their size and cellular origin. This heterogeneity could highly impact their biodistribution and clearance route. We further showed that direct labelling of these EVs with ^{99m}Tc was efficient and stable for up to

24 hours. Biodistribution of bone marrow derived EVs was followed and quantified both *ex vivo* and *in vivo* by SPECT/CT and the two approaches yielded very similar results. There are no published studies so far about the biodistribution of bone marrow derived EVs and their entry into and uptake by the bone marrow and lymphoid system. In concordance with other publications analysing biodistribution of EVs of various sources, we showed that a significant fraction accumulated in the liver, spleen and lungs, most probably in a non-specific manner. We could also show their stable presence in the bone marrow, thymus and lymph nodes, which raises the possibility of a specific uptake of these EVs by the haematopoietic system. Whether intravenously injected bone marrow derived EV clearance is solely non-specific or a tissue-specific uptake can also influence their biodistribution remains to be determined and further, focused studies are needed in this direction.

ACKNOWLEDGMENT

This work was supported by the European Union FP7 DoReMi 249689 grant.

REFERENCES

ANGHILERI, L.J., FIRUSIAN, N., and BRUCKSCH, K.P. (1976). In vivo distribution of 99mTc-labeled liposomes. J Nucl Biol Med, 20: 165-167.

ANDALOUSSI, S., MAGER, I., BREAKEFIELD, X.O., and WOOD, M.J. (2013). Extracellular vesicles: biology and emerging therapeutic opportunities. Nat Rev Drug Discov 12: 347-357.

FRANC, B.L., ACTON, P.D., MARI, C., and HASEGAWA, B.H. (2008). Small-animal SPECT and SPECT/CT: important tools for preclinical investigation. J Nucl Med 49: 1651-1663.

GOLESTANI, R., WU, C., TIO, R.A., ZEEBREGTS, C.J., PETROV, A.D., BEEKMAN, F.J., et al. (2010). Small-animal SPECT and SPECT/CT: application in cardiovascular research. Eur J Nucl Med Mol Imaging 37: 1766-1777.

HONDA, T., KAZEM, I., CROLL, M.N., and BRADY, L.W. (1970). Instant labeling of macro- and microaggregated albumin with 99mTc. J Nucl Med 11: 580-585.

HURLEY, J.H., BOURA, E., CARLSON, L.A., and ROZYCKI, B. (2010). Membrane budding. Cell; 143: 875-887.

HWANG DO, W., CHOI, H., JANG, S.C., YOO, M.Y., PARK, J.Y., CHOI, N.E., et al. (2015). Noninvasive imaging of radiolabeled exosome-mimetic nanovesicle using (99m)Tc-HMPAO. Sci Rep 5: 15636.

IMAI, T., TAKAHASHI, Y., NISHIKAWA, M., KATO, K., MORISHITA, M., YAMASHITA, T., et al. (2015). Macrophage-dependent clearance of systemically administered B16BL6-derived exosomes from the blood circulation in mice. J Extracell Ves 4: 26238

MORISHITA, M., TAKAHASHI, Y., NISHIKAWA, M., SANO, K., KATO, K., YAMASHITA, T., et al. (2015) Quantitative analysis of tissue distribution of the B16BL6-derived exosomes using a streptavidin-lactadherin fusion protein and iodine-125-labeled biotin derivative after intravenous injection in mice. J Pharmac Sci 104: 705-713.

POLYAK, A., HAJDU, I., BODNAR, M., TRENCSENYI, G,, POSTENYI, Z., HAASZ, V. et al. (2013). (99m)Tc-labelled nanosystem as tumour imaging agent for SPECT and SPECT/CT modalities. Int J Pharmac 449: 10-17.

RHODES, B.A. (1991). Direct labeling of proteins with 99mTc. Int J Rad Appl Instrum B 18: 667-676.

SAUNDERSON, S.C. (2015). CD169 mediates the capture of exosomes in the spleen and lymph node (Thesis, Doctor of Philosophy). University of Otago. Retrieved from http://hdl.handle.net/10523/5587

TAKAHASHI, Y., NISHIKAWA, M., SHINOTSUKA, H., MATSUI, Y., OHARA, S., IMAI, T. et al. (2013). Visualization and in vivo tracking of the exosomes of murine melanoma B16-BL6 cells in mice after intravenous injection. J Biotechnol 165: 77-84.

VAN DER POL, E., BOING, A.N., HARRISON, P., STURK, A., NIEUWLAND, R.. (2012). Classification, functions, and clinical relevance of extracellular vesicles. Pharmacol Rev 64: 676-705.

VAN DOMMELEN, S.M., VADER, P., LAKHAL, S., KOOIJMANS, S.A., VAN SOLINGE, W.W., WOOD, M.J. et al. (2012). Microvesicles and exosomes: opportunities for cell-derived membrane vesicles in drug delivery. J Control Release 161: 635-644.

WIKLANDER, O.P., NORDIN, J.Z., O'LOUGHLIN, A., GUSTAFSSON, Y., CORSO, G., MAGER, I., et al. (2015). Extracellular vesicle in vivo biodistribution is determined by cell source, route of administration and targeting. J Extracell Ves 4: 26316.